ORIGINAL RESEARCH

Uncoupling Protein 2 Increases Blood Pressure in DJ-1 Knockout Mice

Carmen De Miguel, PhD; William C. Hamrick, BS; Randee Sedaka, BS; Sudha Jagarlamudi, MD; Laureano D. Asico, DVN; Pedro A. Jose, MD, PhD; Santiago Cuevas, PhD

***Background*—**The redox-sensitive chaperone DJ-1 and uncoupling protein 2 are protective against mitochondrial oxidative stress. We previously reported that renal-selective depletion and germline deletion of *DJ-1* increases blood pressure in mice. This study aimed to determine the mechanisms involved in the oxidative stress–mediated hypertension in *DJ-1*$^{-/-}$ mice.

***Methods and Results*—**There were no differences in sodium excretion, renal renin expression, renal NADPH oxidase activity, and serum creatinine levels between *DJ-1*$^{-/-}$ and wild-type mice. Renal expression of nitro-tyrosine, malondialdehyde, and urinary kidney injury marker-1 were increased in *DJ-1*$^{-/-}$ mice relative to wild-type littermates. mRNA expression of mitochondrial heat shock protein 60 was also elevated in kidneys from *DJ-1*$^{-/-}$ mice, indicating the presence of oxidative stress. Tempol-treated *DJ-1*$^{-/-}$ mice presented higher serum nitrite/nitrate levels than vehicle-treated *DJ-1*$^{-/-}$ mice, suggesting a role of the NO system in the high blood pressure of this model. Tempol treatment normalized renal kidney injury marker-1 and malondialdehyde expression as well as blood pressure in *DJ-1*$^{-/-}$ mice, but had no effect in wild-type mice. The renal *Ucp2* mRNA expression was increased in *DJ-1*$^{-/-}$ mice versus wild-type and was also normalized by tempol. The renal-selective silencing of *Ucp2* led to normalization of blood pressure and serum nitrite/nitrate ratio in *DJ-1*$^{-/-}$ mice.

***Conclusions*—**The deletion of *DJ-1* leads to oxidative stress–induced hypertension associated with downregulation of NO function, and overexpression of *Ucp2* in the kidney increases blood pressure in *DJ-1*$^{-/-}$ mice. To our knowledge, this is the first report providing evidence of the role of uncoupling protein 2 in blood pressure regulation. **(*J Am Heart Assoc*. 2019;8:e011856. DOI: 10.1161/JAHA.118.011856.)**

Key Words: DJ-1 • hypertension • oxidative stress • renal disease • *Ucp2*

Cardiovascular diseases are the leading cause of mortality and morbidity worldwide, especially in patients with chronic kidney disease.[1] Hypertension, the most prevalent cardiovascular risk factor, is known to be associated with oxidative stress.[2] However, hypertension can be both a cause and a consequence of oxidative stress (eg, reactive oxygen species [ROS] and reactive nitrogen species).[2] DJ-1, also known as PARK-7, is a multifunctional oxidative stress response protein that functions as a redox-sensitive chaperone with intrinsic antioxidant properties, especially in the mitochondria, and regulates the expression of several antioxidant genes such as Hsp70 and glutathione.[3,4] Although originally associated with Parkinson's disease, DJ-1 is expressed not only in brain, but also in heart, kidney, liver, pancreas, and skeletal muscle in rodents and humans.[5] DJ-1 is present mainly in the cytoplasm and, to a lesser extent, in the mitochondria. However, following an oxidative challenge, there is increased translocation of DJ-1 into the mitochondria, resulting in the protection of mitochondrial function.[6]

Our group reported that the anti-oxidant and anti-inflammatory properties of the dopamine 2 receptor (D_2R) are mediated in part by DJ-1.[7–9] Renal-selective silencing of DJ-1 in mice, via the renal subcapsular infusion of *DJ-1* siRNA, impairs the D_2R-mediated antioxidant response.[9,10] In addition, mice with *DJ-1* selectively silenced in the kidney and mice with germline deletion of *DJ-1* (*DJ-1*$^{-/-}$) develop high blood pressure (BP), associated with decreased expression and activity of nuclear factor erythroid 2–related factor 2 in the kidney,[10] suggesting that DJ-1 can inhibit renal ROS production, at least in part, via the activation of nuclear factor erythroid 2–related factor 2–regulated antioxidant genes.

From the Section of Cardio-Renal Physiology and Medicine, Division of Nephrology, Department of Medicine, University of Alabama at Birmingham, AL (C.D.M., W.C.H., R.S.); Division of Renal Diseases & Hypertension, Department of Medicine, The George Washington University School of Medicine and Health Sciences, Washington, DC (S.J., L.D.A., P.A.J.); Research Center for Translational Science, Children's National Health System, Washington, DC (S.C.).

Correspondence to: Santiago Cuevas, PhD, Research Center for Genetic Medicine, Children's National Health System, 111 Michigan Av NW, Washington, DC 20010. E-mail: scuevas@childrensnational.org

Received February 20, 2019; accepted March 29, 2019.

© 2019 The Authors. Published on behalf of the American Heart Association, Inc., by Wiley. This is an open access article under the terms of the Creative Commons Attribution-NonCommercial-NoDerivs License, which permits use and distribution in any medium, provided the original work is properly cited, the use is non-commercial and no modifications or adaptations are made.

Clinical Perspective

What Is New?

- This is the first report showing the mechanism involved in hypertension associated with DJ-1 depletion and identifies the novel role of uncoupling protein 2 in blood pressure regulation.

What Are the Clinical Implications?

- These data describe a new mechanism of the regulation of blood pressure and its possible implication in the pathogenesis of essential hypertension, and identify DJ-1 and uncoupling protein 2 as new possible targets for future new approaches to treatment of hypertension and renal diseases.

Uncoupling proteins (UCPs) facilitate the transfer of anions from the inner to the outer mitochondrial membrane, as well as the return of protons to the electron transport chain. It was recently demonstrated that the main function of UCP2 is the control of mitochondria-derived ROS production.[11] Increased expression of UCP2 by peroxisome-proliferator-activated receptor β/δ activation ameliorates the lipopolysaccharide–human cardiomyocyte-induced endothelial dysfunction in mice, associated with a reduction in intracellular oxidative stress.[12] Upregulation of UCP2 expression also protects from the mitochondrial damage induced by high glucose.[13] UCP2 may be effective in treating diabetic vascular complications by decreasing ROS production by the mitochondria.[14] However, depletion of *Ucp2* in mice attenuates the cardiac hypertrophy induced by transverse aortic constriction.[15] Although UCP2 acts to protect the liver against elevated ROS production during drug-induced hepatotoxicity,[16] it also induces chronic depletion of ATP, which can increase the susceptibility of the hepatocytes to ischemia–reperfusion injury in acute energy demand conditions.[17] Therefore, UCP2 has antioxidant properties but, depending upon the concentration, duration of activation, and environmental conditions, UCP2 may also have deleterious effects on physiological functions.[15,17] The main purpose of this study was to determine the mechanism(s) involved in the development of the high BP associated with depletion of *DJ-1.*

Materials and Methods

The data that support the findings of this study are available from the corresponding author upon reasonable request.

DJ-1 Deficient (*DJ-1*$^{-/-}$) Mice

The original F2 hybrid strain (129/SvXC57Bl/6J, Oregon Health Sciences University) containing the mutated *DJ-1* allele (*DJ-1*$^{-/-}$) was backcrossed to wild-type C57Bl/6J for >20 generations and genotyped. All mice were obtained from Jackson Laboratory (Bar Harbor, ME) and were bred in the Animal Care Facility of George Washington University. Male *DJ-1*$^{-/-}$ mice and wild-type littermates were studied at 6 to 8 weeks of age. All studies were approved by the Animal Care and Use Committee of George Washington University. Mice were housed in metabolic cages the day before BP measurement for collection of 24-hour urine samples.

BP Measurement

For measuring BP, we use the Cardiomax-II system (Columbus Instruments International, Columbus, OH), which is a thermodilution cardiac output computer that has been validated for physiological data acquisition system. It is intended to be used on a variety of laboratory animals such as mice to measure BP. Mice were anesthetized with pentobarbital (50 mg/kg IV) and catheters were inserted into the femoral vessels for fluid administration and BP monitoring. Systolic BP was recorded 1 hour after the induction of anesthesia, when the BP was stable. Mice were euthanized (pentobarbital 100 mg/kg, ip) at the conclusion of the study and organs were harvested and flash-frozen, for analysis.

Acute Renal-Selective Downregulation of *Ucp2*

Renal cortical *Ucp2* was silenced by the renal subcapsular infusion of specific siRNA, via an osmotic minipump.[9,10] In brief, adult male C57Bl/6J mice were uninephrectomized 1 week before the implantation of osmotic minipumps. For implantation of the minipumps, mice were anesthetized with pentobarbital (50 mg/kg body weight, ip). Osmotic minipumps (ALZET® Osmotic Pump, Cupertino, CA; 100 µL; flow rate 0.5 µL/hour for 7 days) were filled with previously validated *DJ-1*-specific siRNA (delivery rate, 3 µg/day) or nonsilencing siRNA, as control dissolved in transfection reagent (TransIT® In Vivo Gene Delivery System; Mirus Bio LLC, Madison, WI) under sterile conditions. Each minipump was fitted with polyethylene delivery tubing (Alzet #0007701, Cupertino, CA) and the tip of the tubing was inserted within the subcapsular space of the remaining kidney. Surgical glue was applied at the puncture site to hold the tube in place and prevent extrarenal leakage. The osmotic pump was sutured to the abdominal wall to prevent excessive movement.[9,10]

Treatment With Tempol

DJ-1$^{-/-}$ mice and wild-type littermates were treated with tempol (6 mmol/L) in the drinking water or regular water for 2 weeks.[18] Fresh tempol was dissolved in water every day and protected from light. After 2 weeks of treatment, mice were housed in metabolic cages for 24-hour urine collection. At the end of the urine collection period, mice were anesthetized and BP was measured as described above.

Immunoblotting

Mouse kidney homogenates were subjected to immunoblotting, as previously reported.[7] The primary antibodies used were polyclonal rabbit anti-DJ-1 (Novus, Boston, MA), polyclonal rabbit anti-Nox2 (BioLegend, San Diego, CA), polyclonal goat anti-Nox4 (Abcam, Cambridge, MA), polyclonal rabbit anti-nitro-tyrosine (Cell Signaling, Danvers, MA), polyclonal rabbit anti-Hsp60 (Abcam), and monoclonal mouse anti-GAPDH (Millipore-Sigma Darmstadt, Germany). The densitometry values were normalized by the expression of GAPDH and quantified by Imagen Studio Lite software.

Determination of NADPH Oxidase Activity

NADPH oxidase activity was determined by measuring NADPH-induced chemiluminescence in the presence of lucigenin (5 μmol/L, Invitrogen) and NADPH (100 mol/L, ICN Biomedicals),[19] following manufacturer's instructions. The specificity of the NADPH-dependent superoxide anion production was verified by treatment with diphenylene iodinium (Sigma).

Measurement of Hydrogen Peroxide Concentration

Hydrogen peroxide (H_2O_2) concentration in the kidney was quantified using the Amplex® Red Hydrogen Peroxide/Peroxidase Assay Kit (Thermo Fisher Scientific; catalog number A22188) and following manufacturer's instructions. In brief, 50 μL of standard curve samples, controls, and undiluted kidney homogenates were loaded into a 96-well microplate and 50 μL of the Amplex® Red reagent/HRP working solution was added to each well. The plate was then incubated at room temperature for 30 minutes and protected from light. The plate was then read using an absorbance microplate reader with excitation in the 530 to 560 nm range and emission detection set at 560 nm (Biotek Synergy H1, Winooski, VT).

Immunohistochemical Analysis

Kidneys were fixed in 4% buffered formalin solution overnight at room temperature, transferred into 70% ethanol for 24 hours, and paraffin-embedded. Tissues were cut longitudinally into 4-μm-thick sections and mounted on Superfrost slides. Tissue sections were stained with primary antibodies specific for CD3 (1:600; Abcam), and F4/80 (1:200; Bio-Rad, Hercules, CA), and detected with polymer conjugated secondary antibody (Biocare Medical, Concord, CA). Renal T-lymphocyte and macrophage infiltration was quantified in 10 microscopic fields (200×200 μm, ×400 magnification) in each kidney region (cortex, outer medulla, and inner medulla), with the quantifier blinded from the treatment. The numbers are reported as average of the counts in 10 fields of the kidney section.

Quantitative Reverse Transcription Polymerase Chain Reaction

RNA was extracted from whole renal tissue and cultured MPTCs (Mouse Proximal Tubular Cells), using RNeasy mini kit (Qiagen, Valencia, CA) and quantified by spectrophotometry (NanoDrop ND-1000; Thermo Scientific, Waltham, MA). RNA was reverse transcribed using Quantitect Reverse Transcription kit (Qiagen), according to manufacturer's instructions. The mitochondrial and ER stress primers Nix/BNIP3L,[20] Bnip3,[20] PINK1,[21] PPRC1,[22] Nrf1,[22] PGC1-a,[23] Fis1,[24] Mfn1,[25] Mfn2,[25] Ucp-1,[26] Ucp-2,[26] mtHsp40,[23] mtHSP70,[26] mtHsp60,[24] CHOP,[27] caspase 12,[28] GRP-94,[29] sXBP-1,[30] ATF-4[31], and ATF-6[29] were synthesized by Integrated DNA Technologies (IDT, Coralville, IA; primer sequences are indicated in Table), and primers for *IL-6* (QT00098875), *Ccl2* (QT00167832), *Tnf-α* (QT00104006), and *NfκB* (QT00134421) were purchased from Qiagen. GAPDH and beta-actin were used as housekeeping genes. RNA expression was detected with Quantitect SYBR green kit (Qiagen), using a CFX96 Touch reverse transcription polymerase chain reaction detection system (Bio-Rad).

Analytical Determinations

Levels of renin (Raybiotech, GA; catalog number ELM-Renin1-1), kidney injury marker-1 (KIM-1) (R&D Systems, Minneapolis, MN; catalog number MKM100), and nitrite/nitrate (R&D Systems, Minneapolis, MN, catalog number KGE001) were quantified in urine or serum using the protocols provided by the commercial kits. Malondialdehyde (Cell Biolabs, Inc, San Diego, CA; catalog number STA-332) production was quantified in kidney tissue homogenates using the protocols provided by the commercial kits. Urine sodium concentration was determined by EasyLyte electrolyte analyzer (Medexsupply, Passaic, NJ), and normalized by urine creatinine (Crystal Chem, IL; catalog number 80350) determined by a colorimetric method (Randox, Charles Town, WV). All assays were performed in duplicate.

Statistical Analyses

Data are presented as mean±SEM. Statistical analyses were performed using Sigma Plot 11.0 software (Systat Software, Inc., San Jose, CA). Comparisons between 2 groups used the

Table. Sequences for Mouse Primers Used for Real-Time Polymerase Chain Reaction of the Following Genes: Bnip3, Bnip3l, Pink1, Pprc1, Nrf-1Pgc1-a, Fis1, Mfn 1, Mfn 2, UCPs, Hsp, CHOP, GRP94, sXBP-1, ATF-4, and ATF-6

Gene	Mouse Sequence
Nix/BNIP3L	F: CCT CGT CTT CCA TCC ACA AT[20]
	R: GTC CCT GCT GGT ATG CAT CT
Bnip3	F: GCT CCC AGA CAC CAC AAG AT[20]
	R: TGA GAG TAG CTG TGC GCT TC
PINK1	F: GCT GAT CGA GGA GAA GCA G[21]
	R: GAT AAT CCT CCA GAC GGA AGC
PPRC1	F: TGC CTT GCA GTT ACT CAT GC[22]
	R: CTG ACT TGC ACT GGC AGG TA
Nrf1	F: TGG TCC AGA GAG TGC TTG TG[22]
	R: TTC CTG GGA AGG GAG AAG AT
PGC1-a	F: CCG TAA ATC TGC GGG ATG ATG[23]
	R: CAG TTT CGT TCG ACC TGC GTA A
Fis1	F: AGG CCG TGC TGA ACG AGC TG[24]
	R: GGT AGT TGC CCA CGG CCA GG
Mfn1	F: TGG TCA CAC AAC CAA CTG CT[25]
	R: ACC AAT GCC TTT GCA AGT TGT
Mfn2	F: GGG GCC TAC ATC CAA GAG A[25]
	R: AAA AAG CCA CCT TCA TGT GC
Ucp-1	F: TAT CAT CAC CTT CCC GCT G[26]
	R: GTC ATA TGT TAC CAG CTC TG
Ucp-2	F: TCT ACA ATG GGC TGG TCG C[26]
	R: CAA GCG GAG AAA GGA AGG C
mtHsp40	F: GCC TGT ATG AGA CAA TCA ATG TGA CGA[23]
	R: GTG AAT GTA GTG GTC ACC ATA GCC A
mtHSP70	F: CGT GAG CAA CAG ATT GTA ATC CAG T[26]
	R: GCC ATA TTA ACT GCT TCA ACA CGT TC
mtHsp60	F: TCA TCG GAA GCC ATT GGT CAT A[24]
	R: GCT TTG ACT GCC ACA ACC TGA A
CHOP	F: ATA TCT CAT CCC CAG GAA ACG[27]
	R: TCT TCC TTG CTC TTC CTC CTC
Caspase 12	F: ATG CTG ACA GCT CCT CAT GGA[28]
	R: TGA GAG CCA GAC GTG TTC GT
GRP-94	F: TGG GTC AAG CAG AAA GGA G[29]
	R: TCT CTG TTG CTT CCC GAC TT
sXBP-1	F: GAG TCC GCA GCA GGT G[30]
	R: GTG TCA GAG TCC ATG GGA
ATF-4	F: GCA AGG AGG ATG CCT TTT C[31]
	R: GTT TCC AGG TCA TCC ATT CG
ATF-6	F: TGG GAG TGA GCT GCA AGT GT[29]
	R: ATA AGG GGG AAC CGA GGA G

Bcl2 Interacting Protein 3 (Bnip3), Bcl2 Interacting Protein 3 Like (Bnip3l), PTEN-Induced Putative Kinase 1 (Pink1), Peroxisome Proliferator-Activated Receptor Gamma Coactivator-Related 1 (Pprc1), Nuclear Respiratory Factor 1 (Nrf-1), Peroxisome Proliferator-Activated Receptor Gamma Coactivator 1 Alpha (Pgc1-a), Fission Mitochondrial 1 (Fis1), Mitofusin 1 (Mfn 1), Mitofusin 2 (Mfn 2), Uncoupling Proteins (UCPs), Mitochondrial Heat Shock Protein (Hsp), C/EBP-Homologous Protein (CHOP), Caspase 12, Glucose-Regulated Protein (GRP94), Activating Splice X Box-Binding Protein 1 (sXBP-1), Transcription Factor 4 (ATF-4), and Activating Transcription Factor 6 (ATF-6).

Student *t* test. One-way ANOVA, followed by post hoc analysis using the Holm-Sidak multiple comparison test, was used to assess significant differences among 3 or more groups, and 2-way ANOVA with an interaction term included and a post hoc Bonferroni test was used when comparing more than 2 factors. $P<0.05$ was considered statistically significant.

Results

DJ-1$^{-/-}$ Mice Present Oxidative Stress–Dependent Hypertension

Our group has previously reported that renal *DJ-1* depletion results in oxidative stress–dependent hypertension.[9,10] *DJ-1*$^{-/-}$ mice presented a significant reduction of body weight (Figure 1A). Systolic and diastolic BP as well as renal expression of nitro-tyrosine were elevated, indicating the presence of oxidative stress in the kidney (Figures 1B and 1C). However, serum creatinine was not affected by germline deletion of *DJ-1* (Figure 1D). Renal expression of NADPH oxidase type 2 (Nox2) and type 4 (Nox4) as well as renal NADPH oxidase activity (Figure 1E) and extracellular hydrogen peroxide (H_2O_2) concentration (Figure 1F) were also similar between *DJ-1*$^{-/-}$ and wild-type mice. Additionally, sodium excretion corrected by urine creatinine (Figure 1G) was similar between the genotypes. Taken together, these results indicate that the exaggerated BP and renal oxidative stress associated with DJ-1 depletion are independent of NADPH oxidase activity and renal sodium transport.

Treatment With Tempol Decreases BP and Renal Levels of Malondialdehyde and KIM-1 in *DJ-1*$^{-/-}$ Mice and Increases the Serum Nitrite/Nitrate Ratio

Treatment with tempol, a nitroxide and superoxide dismutase mimetic,[18] normalized BP (tempol:118±2% versus 100±1%,

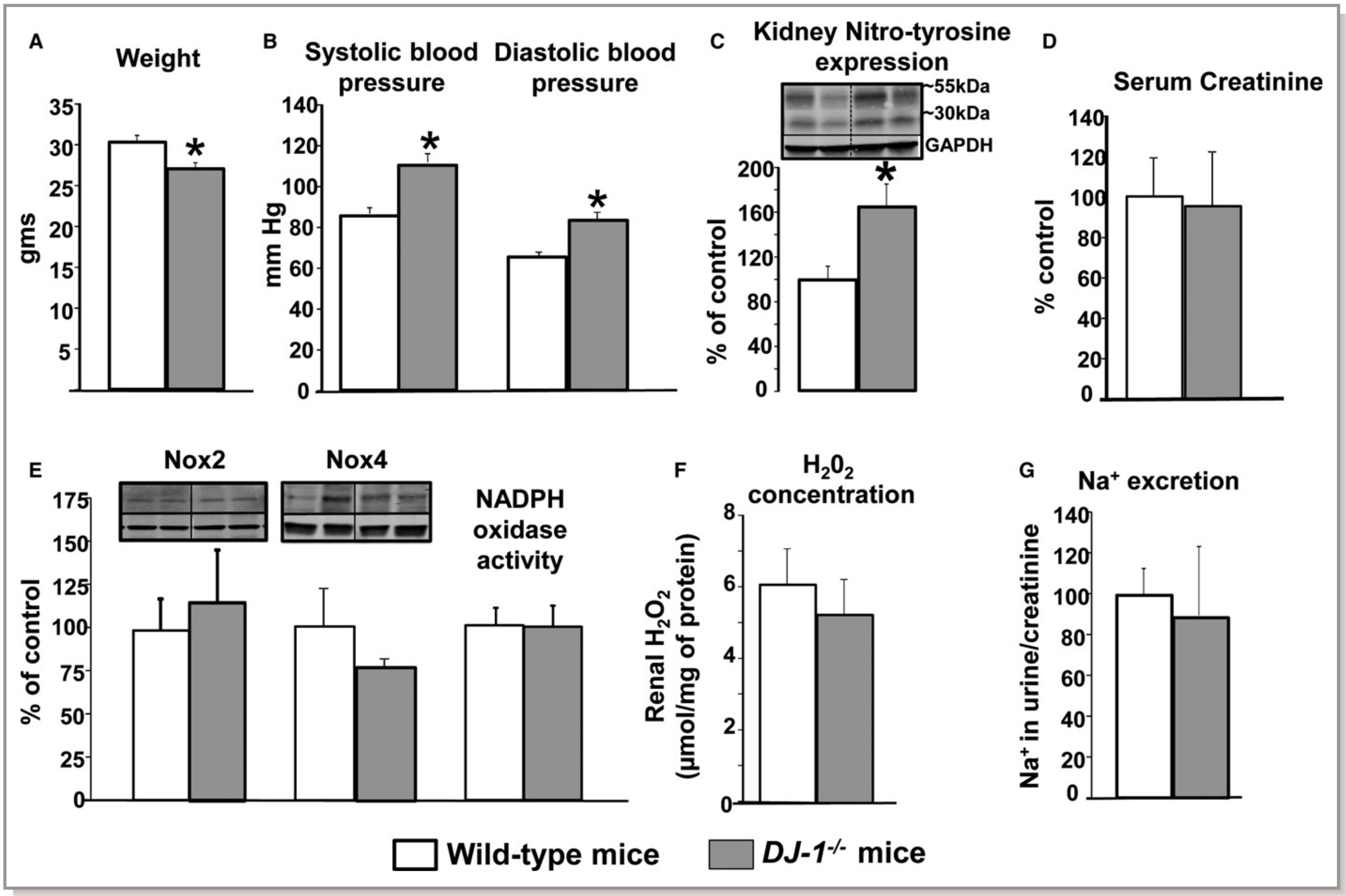

Figure 1. Effect of DJ-1 deletion on BP, oxidative/nitrosative stress, Nox expression and activity, and sodium handling. **A**, *DJ-1*$^{-/-}$ mice are smaller than wild-type littermates. **B**, Systolic BP was measured (Cardiomax II) from the aorta, via the femoral artery, under pentobarbital anesthesia. **C**, Renal homogenates were immunoblotted using antibodies against nitro-tyrosine. Data were normalized by GAPDH. Data are expressed as mean±SEM, n=5 to 8/group. **P*<0.05 vs wild-type littermates, *t* test. **D**, Serum creatinine concentration was determined by Randox colorimetric method. Data are expressed as mean±SEM, n=5 to 8/group; there are no significant differences among the groups. **E**, Renal homogenates were immunoblotted using antibodies against *Nox2* and *Nox4*. Data were normalized by GAPDH. NADPH oxidase activity (light units per milligram of protein) was determined by lucigenin (5 µmol/L) assay. **F**, H_2O_2 expression was determined by Amplex red in renal homogenates. Data are expressed as mean±SEM, n=4/group. **G**, Urine sodium excretion was determined by EasyLyte electrolyte analyzer, and normalized by creatinine. Data are expressed as mean±SEM, n=4/group. There are no significant differences among the groups. BP indicates blood pressure; Nox, NADPH oxidase.

n=4) and renal malondialdehyde production (tempol: 160±23% versus 109±15% versus wild-type, n=4) in *DJ-1*$^{-/-}$ mice, but had no effect in their wild-type littermates (Figure 2A). By contrast, treatment with tempol led to increased serum nitrite/nitrate levels in *DJ-1*$^{-/-}$ mice (+72±30%, n=4) (Figure 2B), suggesting that the nitric oxide system may be involved in the pathogenesis of hypertension in this animal model. Levels of serum renin were not changed by tempol; thus, hypertension in *DJ-1*$^{-/-}$ mice is renin–angiotensin system–independent (Figure 2C). However, urinary excretion of the KIM-1 was increased in *DJ-1*$^{-/-}$ mice (148±22% of wild-type mice, n=4) and decreased by treatment with tempol (−58±3%, n=4) (Figure 2D), indicating that the renal injury induced by the lack of DJ-1 is associated with increased ROS production. Importantly, whole body deletion of *DJ-1* does not lead to renal morphology changes (Figure 2E). We speculate that the nitric oxide (NO) system is involved in the hypertension associated with germline deletion of DJ-1 (Figure 2F).

Deletion of DJ-1 Does Not Result in Exaggerated Renal Inflammation

To assess whether *DJ-1*$^{-/-}$ mice deletion leads to changes in renal inflammation, we analyzed the mRNA expression of *IL-6*, *Tnf*-α, *Mcp-1*, and *NfκB* (Figure 3), as well as renal infiltration of macrophages (Figure 4) and T lymphocytes (Figure 5) in kidneys of *DJ-1*$^{-/-}$ and wild-type mice treated with vehicle or tempol. We found no differences between the groups, indicating that, despite the presence of oxidative stress and

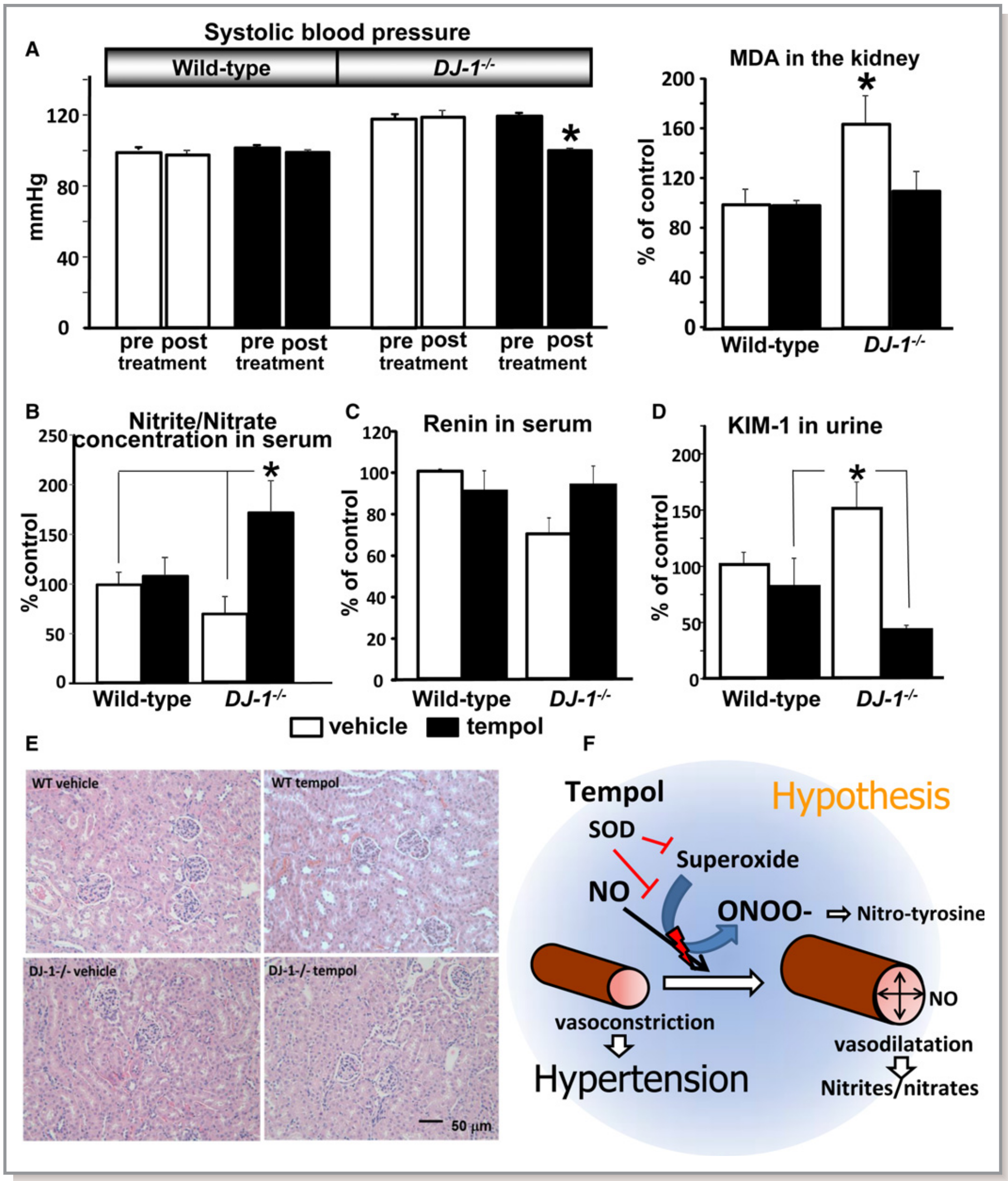

Figure 2. Effect of germline DJ-1 deletion on BP, renal MDA, serum nitrite/nitrate ratio, serum renin concentration, and KIM-1. Tempol treatment normalized the BP and MDA values in *DJ-1*$^{-/-}$ mice. **A**, Systolic BP in *DJ-1*$^{-/-}$ mice. Systolic BP was measured (Cardiomax II) from the aorta, via the femoral artery, under pentobarbital anesthesia in *DJ-1*$^{-/-}$ mice and wild-type littermates (n=4/group). The mice were treated with tempol (6 mmol/L) or vehicle added to the drinking water for 2 weeks. pre=BP values before treatment; post=BP values after treatment. MDA concentration (corrected for protein concentration) in kidney homogenates was measured using a commercial kit (Cell Biolabs, Inc). Data are expressed as mean±SEM, n=4/group.*P<0.05 vs others groups, 1-way ANOVA. **B** through **D**, Serum nitrite/nitrate and renin, and urinary KIM-1 were quantified by ELISA commercial kits. Data are expressed as mean±SEM, n=4/group.*P<0.05 vs others groups, 1-way ANOVA. **E**, Kidney sections of wild-type and *DJ-1*$^{-/-}$ mice treated with tempol were stained with hematoxylin and eosin. No differences were found between the 2 mouse strains. **F**, Proposed mechanism of action of tempol to prevent *DJ-1*$^{-/-}$ deletion-mediated hypertension: tempol increases the NO bioavailability by preventing its conversion to peroxynitrite and nitro-tyrosine and resulting in increased vasodilatation and nitrite/nitrate serum concentration and decreased BP. BP indicates blood pressure; KIM-1, kidney injury molecule-1; MDA, malondialdehyde; NO, nitric oxide; ONOO, Nitro-tyrosine; SOD, superoxide.

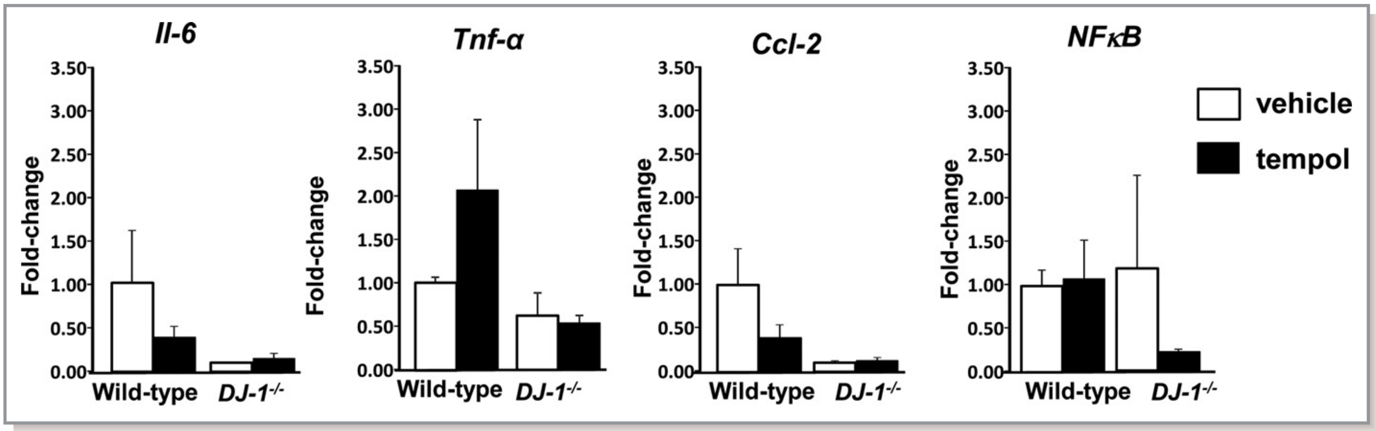

Figure 3. Renal inflammatory cytokines are not altered in *DJ-1*$^{-/-}$ mice. Wild-type mice were treated with tempol or vehicle as described in Figure 2. Kidney mRNA expression of interleukin-6 (*Il-6*), tumor necrosis factor alpha (*Tnf-α*), chemokine (C-C motif) ligand 2 (*Ccl-2*), and nuclear factor κ-light-chain-enhancer of activated B cells (NFkB) was quantified by quantitative real-time polymerase chain reaction, and normalized by GAPDH. No differences were found between groups. Data are expressed as mean±SE, n=4 per group.

hypertension, *DJ-1*$^{-/-}$ mice do not present exaggerated renal inflammation.

Germline DJ-1 Deletion Increases Heat Shock Protein 60 and UCP2 in the Kidney

Because mitochondria are well-known sources of superoxide and other ROS,[11] we examined the renal expression of different markers of mitochondrial stress in the experimental animals. There were no differences between the groups in the mRNA expression of markers of mitophagy, mitochondrial fusion, and fission or biogenesis between *DJ-1*$^{-/-}$ mice and wild-type (Figure 6A). mRNA expression of mitochondrial heat shock protein 60 (mt*Hsp60*) was elevated in kidneys of *DJ-1*$^{-/-}$ mice (2.9±0.1-fold, n=4), while expression of mt*Hsp40* was not different between the groups (Figure 6B). These results suggest that the lack of DJ-1 expression resulted in mitochondrial stress, likely caused by oxidative redox imbalance. Interestingly, treatment with tempol led to a significant difference in the expression of *mtHsp40* between the genotypes (wild-type+tempol versus *DJ1*$^{-/-}$+tempol: 0.6±0.2 versus 1.2±0.1, n=4), but failed to inhibit the renal mRNA expression of *Hsp60* in *DJ-1*$^{-/-}$ mice. By contrast, the renal expression of *Ucp2*, which decreases the production of superoxide in the mitochondria[11] and was significantly elevated in *DJ-1*$^{-/-}$ mice (4.1±1.1-fold of wild-type, n=4), was normalized by treatment with tempol (Figure 6B). Thus, it is possible that compensatory renal overexpression of *Ucp2* in these animals in response to the lack of DJ-1 could provide an additional protection on mitochondrial function and prevents the development of renal damage.[11,12,15,32] Interestingly, and contrary to our expectations, the protein expression of mtHsp60 in the kidney was not different among the groups, possibly highlighting a time lag in the translation of mRNA to protein in the timeline of our experiments (Figure 6C; $P>0.05$).

Endoplasmic reticulum stress has been closely associated with oxidative stress and mitochondrial stress,[33,34] renal diseases, and hypertension.[35,36] To elucidate the molecular mechanisms involved in the development of hypertension in the *DJ-1*$^{-/-}$ mouse, we measured the mRNA expression of markers of endoplasmic reticulum stress and mitochondrial stress in kidneys of our experimental animals. Renal expression of the endoplasmic reticulum stress markers GRP94, ATF-4, ATF-6, spliced XBP-1, CHOP, and caspase 12 was not different between wild-type and *DJ-1*$^{-/-}$ mice. Furthermore, treatment with tempol did not affect their expression (Figure 7).

Renal-Selective Silencing of *Ucp2* Normalizes BP in *DJ-1*$^{-/-}$ Mice

To better understand the role of Ucp2 in the control of BP and, possibly, kidney injury, *Ucp2* expression was silenced specifically in the kidney of *DJ-1*$^{-/-}$ mice and wild-type littermates, via renal subcapsular infusion of *Ucp2 siRNA*.[9,10] The efficiency of *Ucp2* silencing by *Ucp2 siRNA* infusion into the kidney was determined by quantitative polymerase chain reaction, and we determined that it was similar in both genotypes (nonspecific siRNA versus *Ucp2*: wild-type −0.63±0.07-fold and *DJ1*$^{-/-}$ −0.60±0.06-fold) (Figure 8A).

Specific renal silencing of *Ucp2* normalized BP in *DJ-1*$^{-/-}$ mice when compared with mice transfected with nonsilencing siRNA (*DJ-1*$^{-/-}$ *mice*: 122±5 versus 98±7 mm Hg, n=4) (Figure 8B) after 7 days of infusion, indicating that increased renal *Ucp2* expression is involved in the increased BP associated with germline depletion of DJ-1. In a separate set of

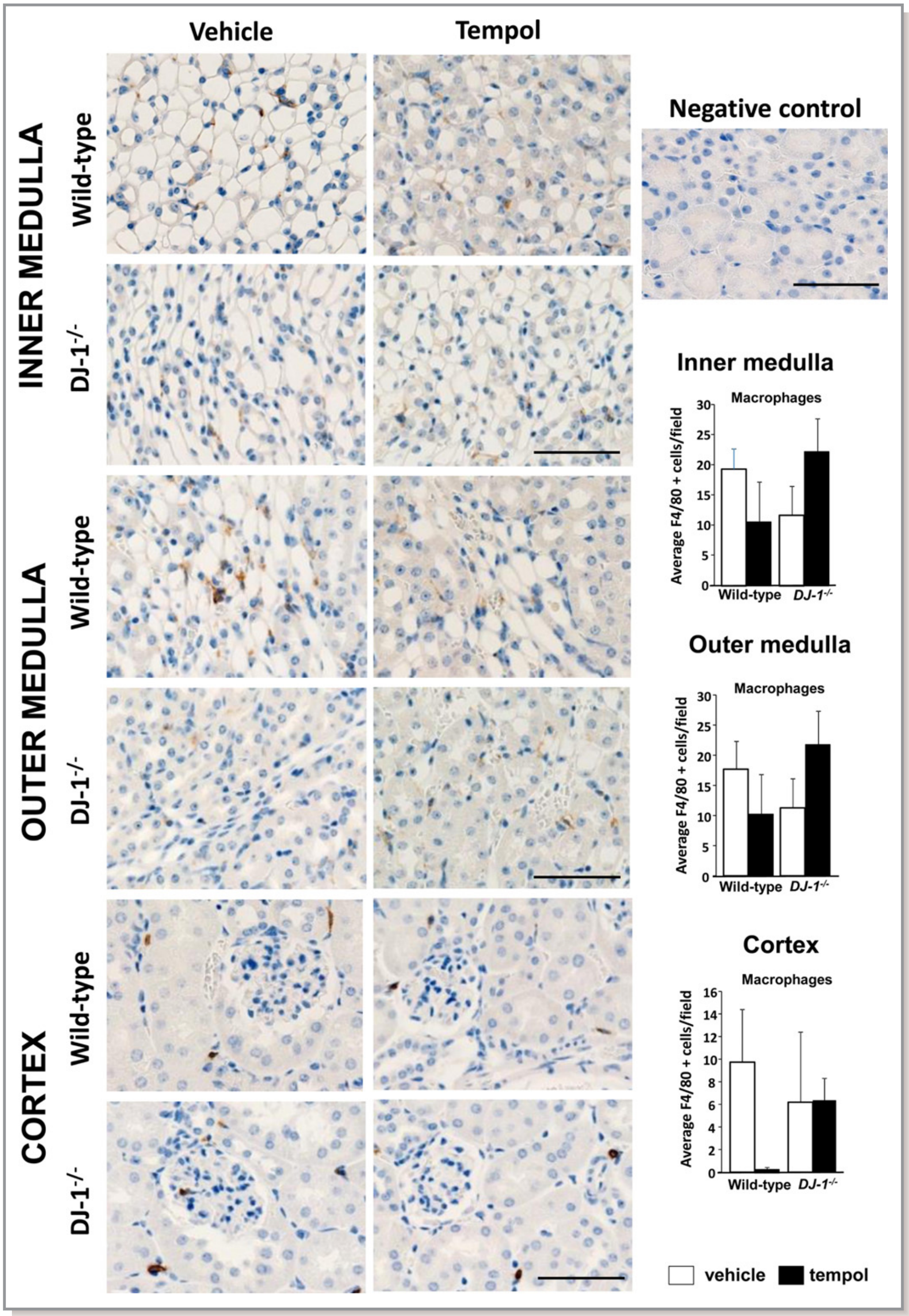

Figure 4. Renal infiltration of macrophages is not different among the groups. Macrophages were immunostained with antibodies directed against F4/80 in renal sections. F4/80$^+$ cells (brown cells in the images) were quantified in the renal cortex and outer and inner medulla of *DJ-1*$^{-/-}$ and wild-type mice treated with vehicle or tempol. Cells were quantified per 400×400 mm field (×400 magnification). No differences were found between groups. Data are expressed as mean±SE, n=4 per group.

animals, long-term renal silencing of *Ucp2* via siRNA infusion for a total of 28 days also normalized the BP values (*DJ-1*$^{-/-}$ *mice*: 120±2 versus 101±1 mm Hg, n=4) (data not shown in figures). Silencing of the *Ucp2* expression in *DJ-1*$^{-/-}$ mice also led to an elevation of the serum nitrite/nitrate concentration, bringing the levels back to normal levels and indicating that

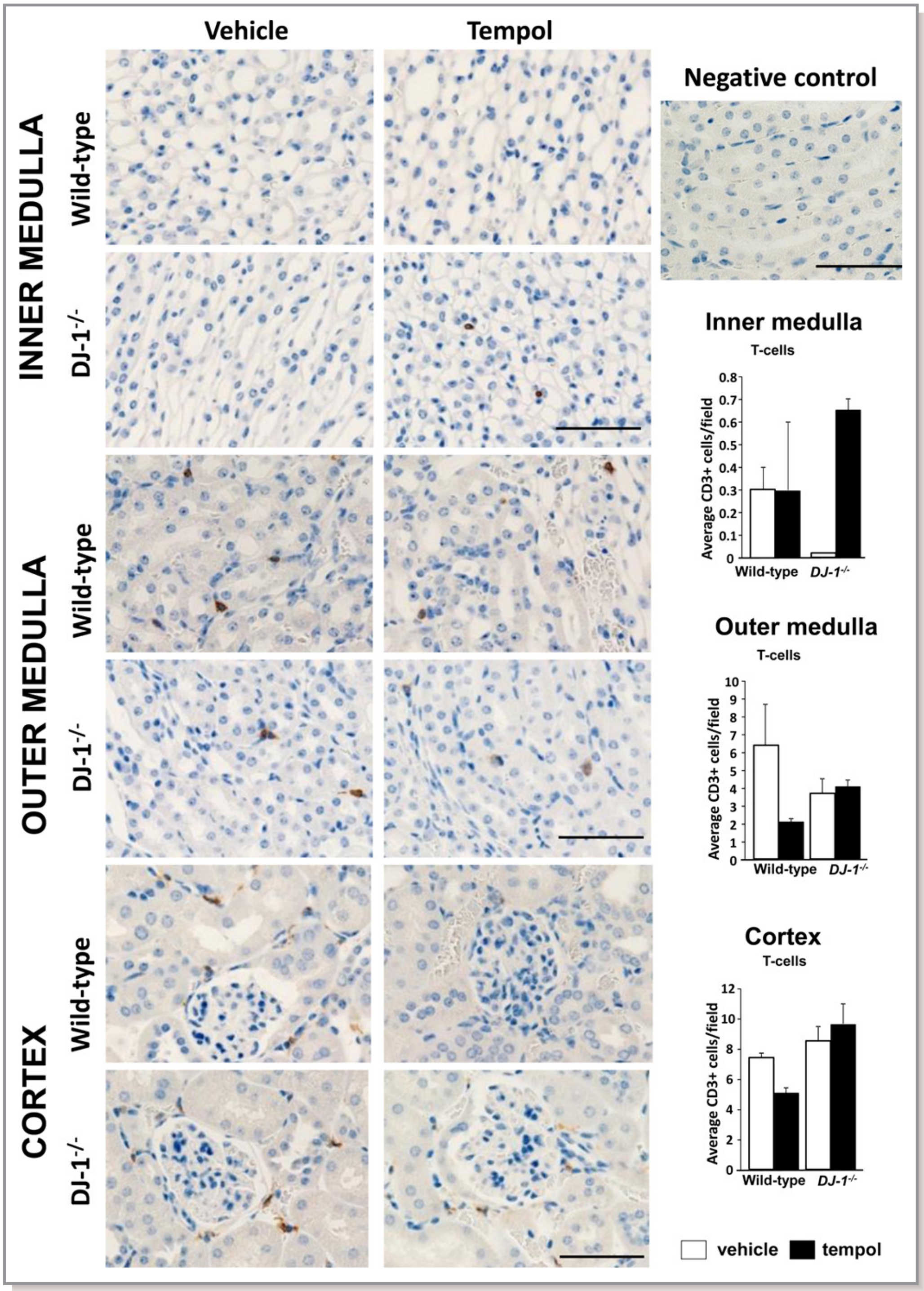

Figure 5. T-cell infiltration in the kidney is not different among the groups. T cells were immunostained with antibodies directed against the cell surface marker CD3 in renal sections. $CD3^+$ cells (brown cells in the images) were quantified in the renal cortex and outer and inner medulla of *DJ-1*$^{-/-}$ and wild-type mice treated with vehicle or tempol. Cells were quantified per 400×400 mm field (×400 magnification). No differences were found between groups. Data are expressed as mean±SE, n=4 per group.

decreased production of NO is involved in the development of elevated BP in *DJ-1*$^{-/-}$ mice (Figure 8C). KIM-1 levels in the kidney were not altered by renal *Ucp2* siRNA infusion and remained elevated in the *DJ-1*$^{-/-}$ mice compared with wild-type littermates (Figure 8D). Similarly, the mRNA expression levels of the mitochondrial stress markers *mtHsp40* and *mtHsp60* in the kidney were not affected by the kidney-specific silencing of *Ucp2* (*mtHsp40*, wild-type nonsilencing siRNA

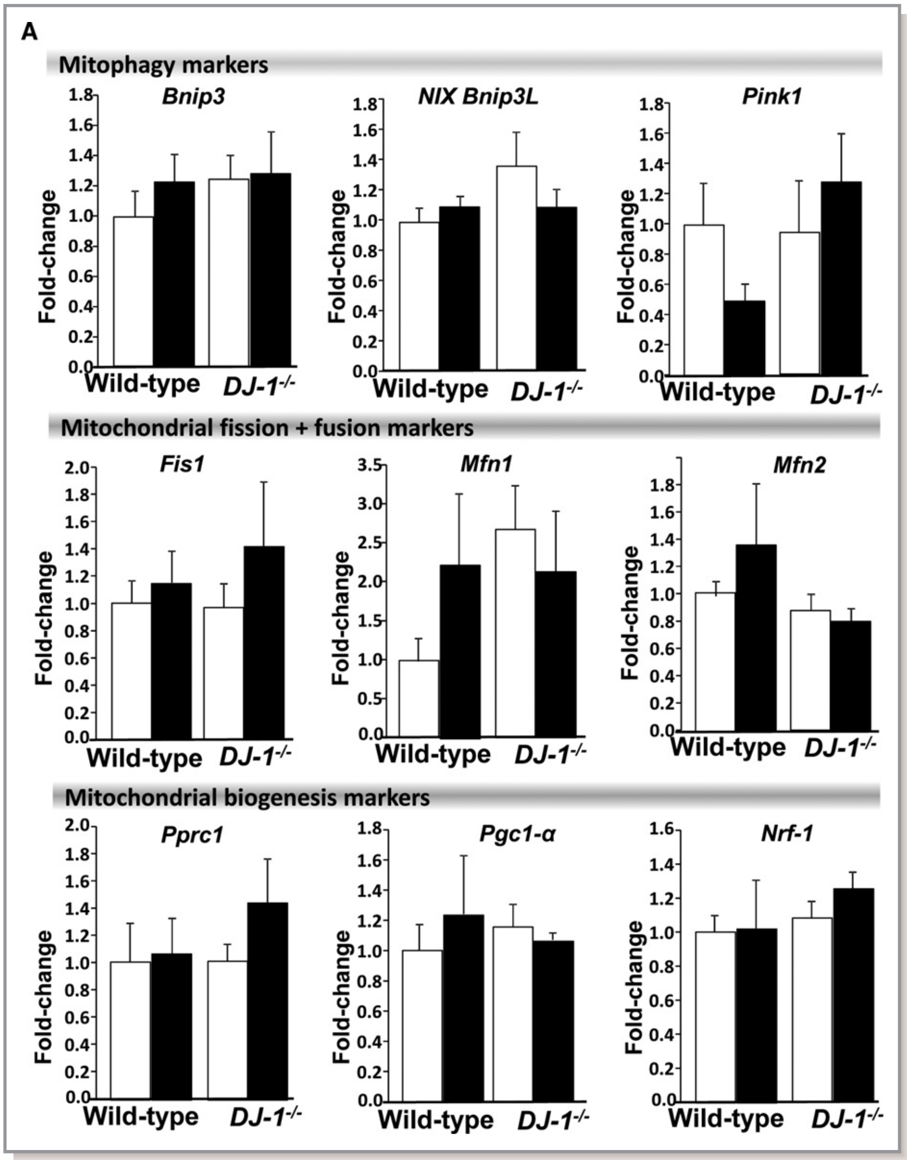

Figure 6. Effect of DJ-1 deletion on mitochondrial oxidative stress. **A** and **B**, mRNA expression the markers of mitophagy; Bcl2 interacting protein 3 (*Bnip3*), Bcl2 interacting protein 3 like (*Bnip3L*), PTEN-induced putative kinase 1 (*Pink1*), the markers of mitochondrial fusion and fission; fission mitochondrial 1 (*Fis1*), mitofusin 1 (*Mfn 1*), mitofusin 2 (*Mfn 2*), mitochondrial biogenesis; peroxisome proliferator-activated receptor γ coactivator-related 1 (*Pprc1*), peroxisome proliferator-activated receptor γ coactivator 1 α (*Pgc1-α*), and nuclear respiratory factor 1 (*Nrf-1*) and mitochondrial heat shock proteins 40 and 60 (*mtHsp40* and *mtHsp60*) as well as uncoupling proteins 2 (*Ucp2*) were determined in kidneys of *DJ-1*$^{-/-}$ mice and wild-type littermates by quantitative real-time polymerase chain reaction and normalized by GAPDH. **C**, mtHsp60 protein expression was assessed by Western blot and normalized by GAPDH protein expression. Data are expressed as mean±SEM, n=4/group. *$P<0.05$ vs wild-type mice; $^{\#}P<0.05$ vs *DJ1*$^{-/-}$ mice treated with vehicle, 2-way ANOVA.

versus *Ucp2* siRNA: 1.0±0.18 versus 1.2±0.33, *DJ-1*$^{-/-}$ nonsilencing siRNA versus *Ucp2* siRNA: 0.9±0.18 versus 0.7±0.15; *mtHsp60*, wild-type nonsilencing siRNA versus *Ucp2* siRNA: 1.0±0.21 versus 1.4±0.41, *DJ-1*$^{-/-}$ nonsilencing siRNA versus *Ucp2* siRNA: 1.0±0.17 versus 0.6±0.19; n=4/group; $P>0.05$) (data not included in the figures).

Discussion

We recently reported that disruption of DJ-1 in mice causes oxidative stress–dependent hypertension.[5,10] We now report that DJ-1 deletion leads to exaggerated reactive nitrogen species production, lipid peroxidation, and renal cortical injury, and results in elevated expression of *Ucp2*

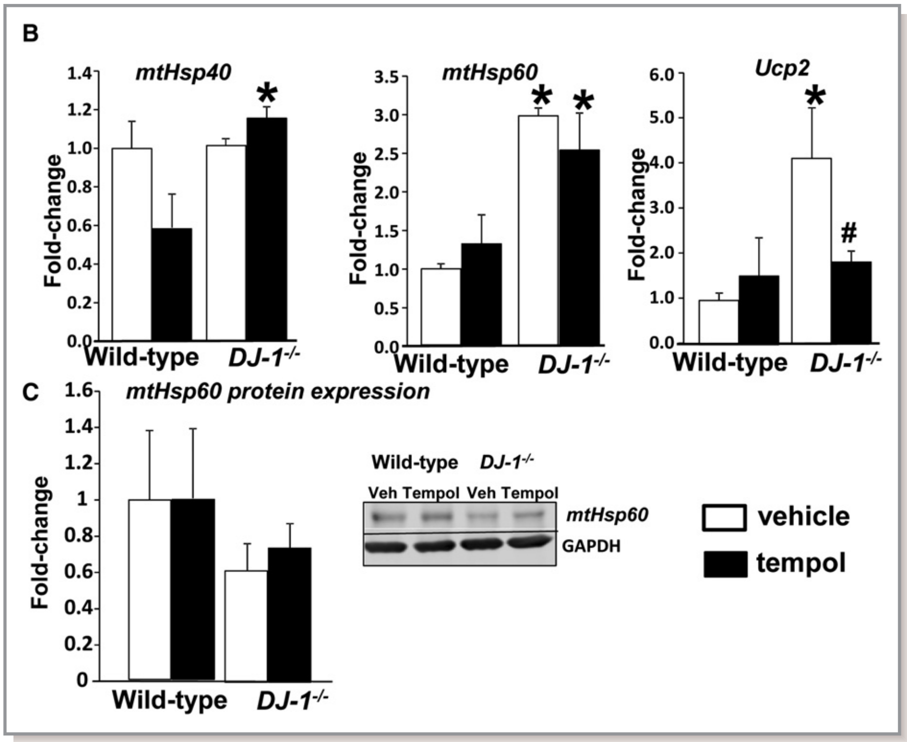

Figure 6. Continued.

in the kidney. We further show that specific silencing of *Ucp2* in the kidney normalizes BP in this experimental model. To our knowledge, this is the first report showing the ability of UCP2 to regulate BP and decrease NO activity.

DJ-1 Depletion Results in Increased Reactive Nitrogen Species and Increased Renal Expression of Ucp2, Which Is Normalized by Treatment With the Antioxidant Tempol

DJ-1 is a peroxiredoxin protein that exerts a protective role against oxidative stress.[37] Our group previously showed that DJ-1 is involved in the antioxidant activity mediated by dopamine 2 receptors, which is mainly associated with their ability to inhibit NADPH oxidase activity.[8,9] Our present studies demonstrate that the oxidative stress–dependent hypertension observed in *DJ-1*$^{-/-}$ mice is independent of changes in NADPH oxidase activity and regulation of renal sodium excretion. We also demonstrate that *DJ1*$^{-/-}$ mice have increased renal levels of nitro-tyrosine, a marker of peroxynitrite production and thus, nitrogen species production.[38] Moreover, nitric oxide production is decreased by germline deletion of DJ-1, as indicated by the decreased serum and renal nitrite/nitrate ratio in *DJ-1*$^{-/-}$ mice. Interestingly, treatment with the antioxidant tempol increases the nitrite/nitrate ratio in the kidney in *DJ-1*$^{-/-}$ mice, suggesting that the hypertension in *DJ-1*$^{-/-}$ mice is caused by NO dysregulation, probably caused by deficient function of the nitric oxidase system and independently of changes in the renal angiotensin system or NADPH oxidase activity. Treatment with tempol also normalizes the excretion of the proximal tubular damage marker KIM-1, indicating that the kidney damage induced by loss of DJ-1 is ROS dependent.

Lack of DJ-1 Function Results in Increased mtHsp60 and Ucp2 Expression in the Kidney

Because DJ-1 has an important role in protecting mitochondrial function,[39,40] and mitochondrial dysfunction has been repeatedly associated with hypertension,[41] the renal mitochondrial status of *DJ1*$^{-/-}$ mice was assessed in animals treated with vehicle or tempol. Significantly elevated expression of mitochondrial heat shock protein 60 (*mtHsp60*) and *Ucp2* was observed in kidneys from *DJ-1*$^{-/-}$ mice treated with vehicle. Elevated levels of unfolded proteins in cellular compartments activate chaperone gene transcription and facilitate the further folding of misfolded proteins into their active conformations.[42] Mitochondria contain several members of the heat-shock protein (mtHsp) family that assist with proteostasis within this organelle and, therefore, help in maintaining mitochondrial function. In particular, *mtHsp60* is expressed in the mitochondrial matrix, and its expression is

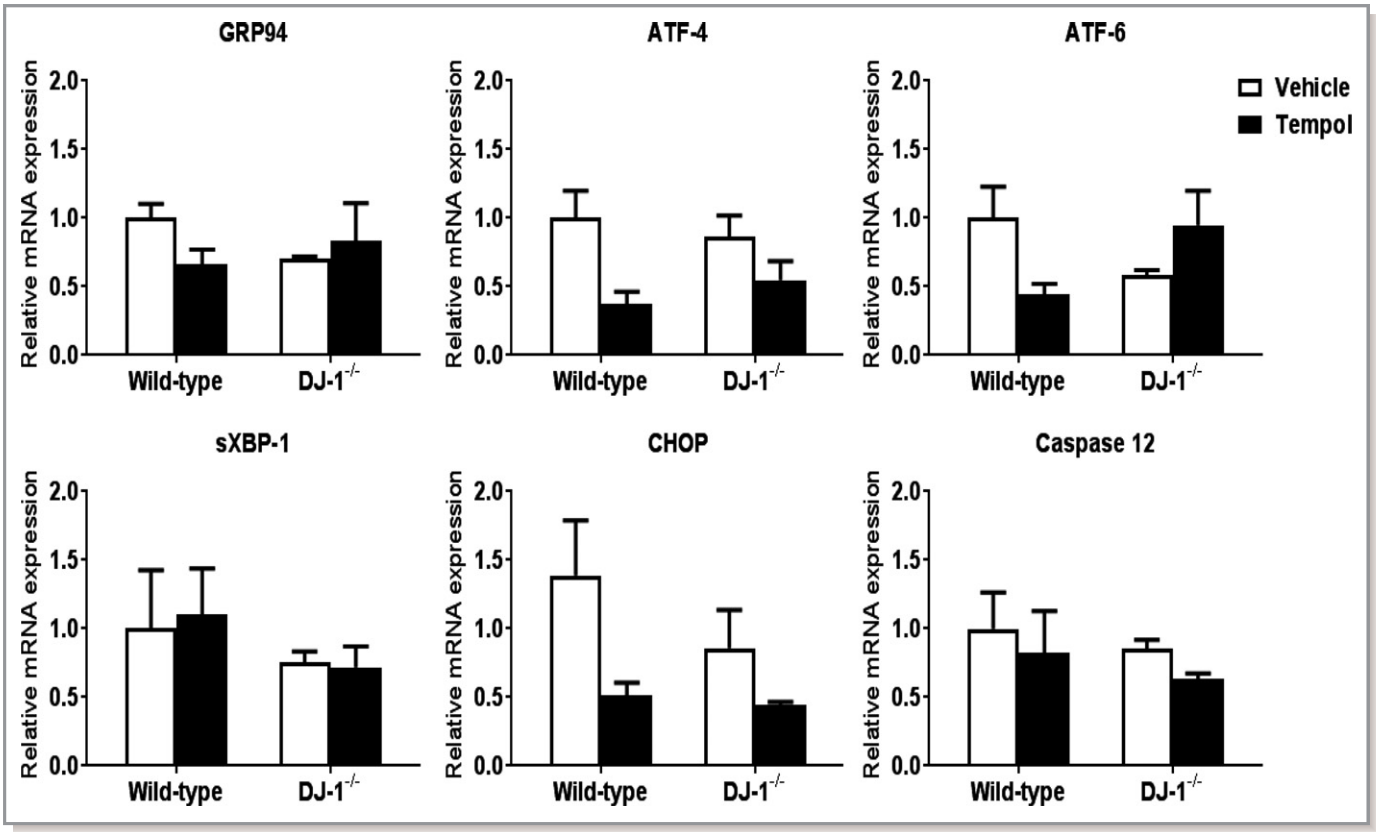

Figure 7. Expression of markers of endoplasmic reticulum stress in the cortex is similar among the genotypes and treatments. mRNA expressions of GRP94 (a chaperone involved in the processing and transport of secreted proteins), ATF-4, ATF-6, sXBP-1, CHOP, and caspase 12 in renal cortex of *DJ-1*$^{-/-}$ mice and wild-type littermates were quantified by quantitative real-time polymerase chain reaction and normalized to GAPDH. n=4/group. No differences were found between the 2 mouse strains. ATF-4 indicates activating transcription factor 4; ATF-6, activating transcription factor 6; CHOP C/EBP-homologous protein; GRP94, glucose-regulated protein; sXBP-1, spliced X box-binding protein 1.

upregulated in response to mitochondrial disorders,[43,44] and thus, it is considered a marker of mitochondrial stress. Increased expression of *mtHsp60* has been associated with cardiovascular diseases,[44,45] diabetes mellitus,[46,47] Alzheimer's disease,[48,49] and cancer.[49] In our studies, treatment with tempol did not decrease the expression of *mtHsp60* in the kidneys of *DJ-1*$^{-/-}$ mice, possibly caused by tempol not specifically targeting the mitochondria. Although we also measured mtHsp60 protein expression, differences were not found between groups. ATP- and ubiquitin-independent 20S proteasome have been reported to play a key role in the selective removal of oxidized proteins[50,51]; therefore we speculate that the overoxidation of mtHsp60 in our experimental animals, likely due the increased the ROS expression in the mitochondria, induces its degradation. The increased degradation of overoxidized mtHsp60 may, in turn, lead to increased mRNA expression caused by a feedback regulation mechanism. We will further investigate this avenue in future studies.

On the other hand, treatment with tempol led to a difference in expression of *mtHsp40* between the genotypes, with the *DJ-1*$^{-/-}$ mice showing significantly greater expression than the wild-type mice. *mtHsp40* has an important role in the maintenance of mitochondrial proteostasis, mainly by aiding with protein refolding.[52] Elwi et al[53] demonstrated an association between dysregulation of *mtHsp40* and mitochondrial fragmentation, and suggested a critical role of this chaperone protein in the modulation of mitochondrial morphology.[54] Tempol has been reported to attenuate ROS-mediated tissue damage,[55] but is not able to protect the mitochondria from an excessive ROS production, and this may induce oxidative stress. Our results demonstrate that treatment with tempol unmasks mitochondrial oxidative stress associated with germline deletion of *DJ-1*$^{-/-}$, as highlighted by the elevated expression of *mtHsp40* and *mtHsp60* in the kidney.

UCPs protect against oxidative stress and attenuate both mitochondrial ROS production[56] and apoptosis in renal ischemia–reperfusion injury.[57] There are 5 subtypes of UCPs: UCP1 to UCP5.[58] UCP2 in particular is highly expressed in the kidney.[59] UCP2 has been reported to regulate mitochondrial dynamics (mitochondrial fission and fusion),[60] as well as to

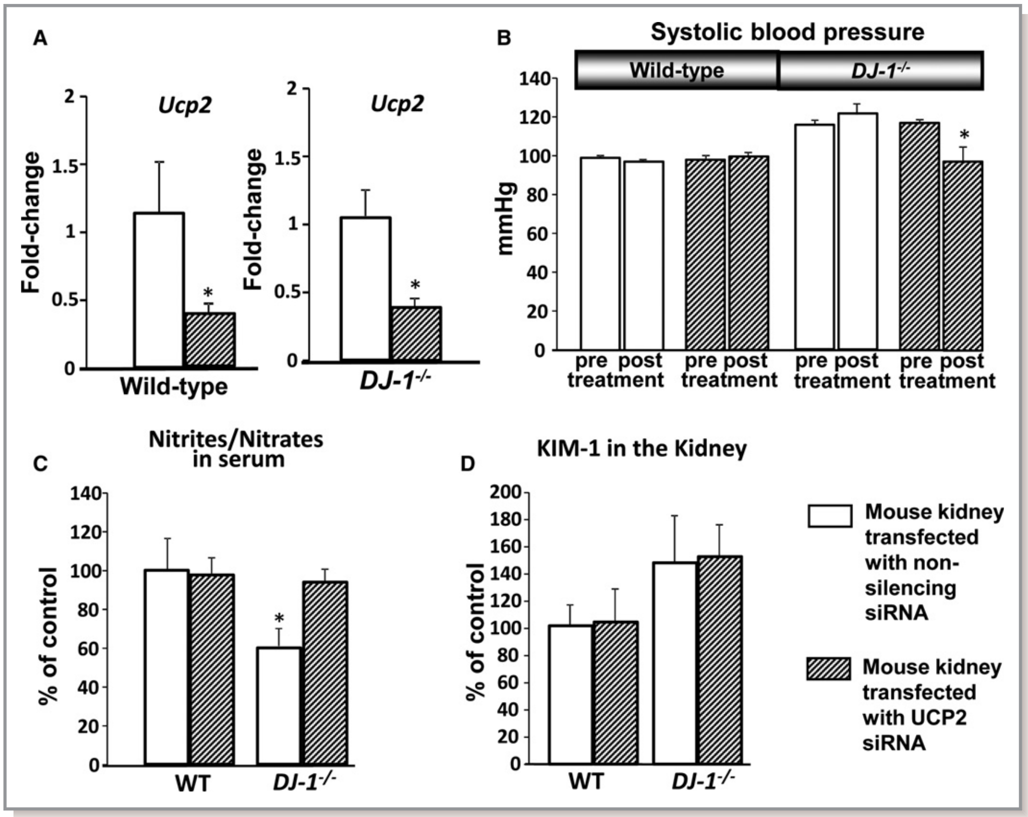

Figure 8. Effect of in vivo renal *Ucp2* silencing on BP, serum nitrite/nitrate, and renal KIM-1. **A**, *DJ-1*$^{-/-}$ mice and wild-type littermates were in vivo transfected with *Ucp2 siRNA* via renal subcapsular infusion. mRNA expression of *Ucp2* was measured in renal homogenates by quantitative real-time polymerase chain reaction and normalized by GAPDH and beta actin. Data are expressed as mean±SEM, n=4/group. **P*<0.05 vs wild-type mice, 1-way ANOVA. **B**, Systolic BP in *DJ-1*$^{-/-}$ mice. Systolic BP was measured (Cardiomax II) from the aorta, via the femoral artery, under pentobarbital anesthesia in *DJ-1*$^{-/-}$ mice and wild-type littermates transfected with *Ucp2* and nonspecific siRNA via subscapular infusion (n=4/group). **C** and **D**, Serum nitrite/nitrate and renal KIM-1 were quantified using a commercial kit. Data are expressed as mean±SEM, n=4/group, **P*<0.05 vs other groups, *t* test and 1-way ANOVA. BP indicates blood pressure; KIM-1, kidney injury molecule-1; *Ucp2*, uncoupling proteins 2.

protect against mitochondrial dysfunction by reducing the release of anion superoxide in the electron transport chain.[61] Moreover, it has been speculated that the antioxidant properties of UCP2 may be caused by its ability to increase the mitochondrial glutathione levels.[62] However, the beneficial effects of UCP2 against oxidative stress remain unclear.[63] UCP2 deficiency in mice is protective against cerebral ischemia following middle cerebral artery occlusion,[62] whereas UCP2 overexpression in the brain prevents stroke and decreases neuronal death.[64] The role of UCP2 in kidney damage is controversial in the literature. While a role for UCP2 in promoting kidney fibrosis has been described in a model of chronic kidney injury,[65] recent reports have unveiled a protective role of UCP2 against the development of kidney ischemia/reperfusion injury through inhibition of tubular apoptosis and induction of autophagy.[57] Our results indicate that a lack of *DJ-1* is associated with upregulation of *Ucp2* in the kidney, and that treatment with tempol normalizes these levels in *DJ-1*$^{-/-}$ mice. *Ucp2* expression is activated by ROS[66]; thus our results suggest that *Ucp2* could have been induced by the increased production of ROS in our hypertensive mouse model. The elevated expression of *mtHsp40* and *mtHsp60* that accompany the upregulation of *Ucp2* in the *DJ-1*$^{-/-}$ model further supports this conclusion.

Ucp2 Overexpression Increases BP in DJ-1$^{-/-}$ Mice

Our results suggest that *Ucp2* is involved in the elevated BP associated with *DJ-1* depletion. It has been reported that long-term *Ucp2* overexpression could induce deleterious effects, instead of its usual beneficial effects. Decreased UCP2 expression would impair its antioxidant properties.[15,17,67] Although the increased renal expression of *Ucp2* in *DJ-1*$^{-/-}$ mice may act as a compensatory mechanism to preserve mitochondrial function in this model, an excessive elevation of

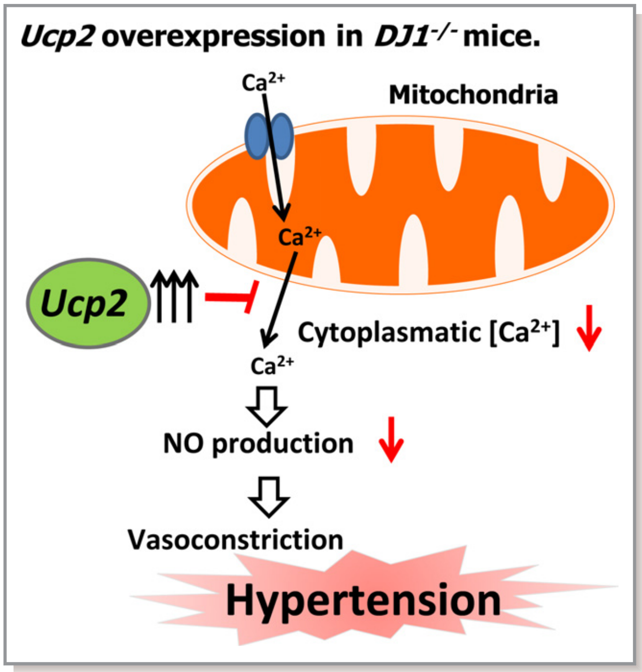

Figure 9. Working hypothesis. Exaggerated *Ucp2* expression in the kidney can disrupt normal mitochondrial Ca^{2+} uptake handling, which could decrease Ca^{2+} uptake in the mitochondria, decreasing NO production and increasing blood pressure. NO indicates nitric oxide; *Ucp2*, uncoupling proteins 2.

Ucp2 expression in the kidney may also lead to decreased nitric oxide production and elevated BP. Renal *Ucp2* expression is increased 5-fold in *DJ-1*$^{-/-}$ mice, and ROS is known to elevate *Ucp2* expression; thus, the exaggerated expression of renal *Ucp2* in our animals could be ROS mediated. This notion is supported by the decreased *Ucp2* expression and normalized BP values in *DJ-1*$^{-/-}$ mice after treatment with tempol. This may indicate that excessive and chronic overexpression of *Ucp2* could have deleterious consequences on BP regulation in *DJ-1*$^{-/-}$ mice, but this effect would not be observed in normal conditions and moderate expression of *Ucp2*.[15,17,67]

It is well established that mitochondria exhibit spatial Ca^{2+} buffering in a distinct area of the cytosol and have a large capacity to accumulate Ca^{2+} and uptake and egress of Ca^{2+}.[68] UCP2 modulates intracellular Ca^{2+} by the regulation of mitochondrial Ca^{2+} uptake.[69] Moreover, elevated expression of UCP2 has negative effects on mitochondrial Ca^{2+} uptake, indicating that upregulation of UCP2 can disrupt normal mitochondrial Ca^{2+} uptake handling[67] and result in enhanced Ca^{2+} sequestration competence of the mitochondria and decreased cytoplasmic Ca^{2+}.[70] It has also been reported that increased cytoplasmic Ca^{2+} leads to increase NO production and improved endothelial function.[71,72] In our experience, silencing *Ucp2* expression in kidneys of *DJ-1*$^{-/-}$ mice normalized the nitrite/nitrate concentration in serum, indicating that the nitric oxide system is critically involved in the hypertension in *DJ-1*$^{-/-}$ mice. We speculate that exaggerated *Ucp2* expression in the kidney could lead to increased Ca^{2+} uptake in the mitochondria, decreasing NO production and, thus, increasing BP (Figure 9). Further experiments are needed to test this working hypothesis.

Perspectives

Our data indicate that an exaggerated and prolonged increase in renal *Ucp2* levels leads to elevated BP in *DJ1*$^{-/-}$ mice, caused by decreased nitric oxide production, suggesting that excessive *Ucp2* expression may have deleterious consequences on BP regulation. Further studies are needed to understand the complex interaction between UCP2 and BP regulation and to establish whether or not modulation of renal DJ-1 and UCP2 function can be a new therapeutic approach in renal diseases and hypertension.

Sources of Funding

These studies were supported in part by NIH T32 DK007545 to De Miguel and NIH/NHLBI 5P01 HL074940-10 and NIH/NIDDK 7R01 DK039308-31 to Jose.

Disclosures

None.

References

1. Tuegel C, Bansal N. Heart failure in patients with kidney disease. *Heart*. 2017;103:1848–1853.
2. Araujo M, Wilcox CS. Oxidative stress in hypertension: role of the kidney. *Antioxid Redox Signal*. 2014;20:74–101.
3. Liu F, Nguyen JL, Hulleman JD, Li L, Rochet JC. Mechanisms of DJ-1 neuroprotection in a cellular model of Parkinson's disease. *J Neurochem*. 2008;105:2435–2453.
4. Zhou W, Freed CR. DJ-1 up-regulates glutathione synthesis during oxidative stress and inhibits A53T alpha-synuclein toxicity. *J Biol Chem*. 2005;280:43150–43158.
5. Nagakubo D, Taira T, Kitaura H, Ikeda M, Tamai K, Iguchi-Ariga SM, Ariga H. DJ-1, a novel oncogene which transforms mouse NIH3T3 cells in cooperation with ras. *Biochem Biophys Res Commun*. 1997;231:509–513.
6. Junn E, Jang WH, Zhao X, Jeong BS, Mouradian MM. Mitochondrial localization of DJ-1 leads to enhanced neuroprotection. *J Neurosci Res*. 2009;87:123–129.
7. Armando I, Wang X, Villar VA, Jones JE, Asico LD, Escano C, Jose PA. Reactive oxygen species-dependent hypertension in dopamine D2 receptor-deficient mice. *Hypertension*. 2007;49:672–678.
8. Cuevas S, Villar VA, Jose PA, Armando I. Renal dopamine receptors, oxidative stress, and hypertension. *Int J Mol Sci*. 2013;14:17553–17572.
9. Cuevas S, Zhang Y, Yang Y, Escano C, Asico L, Jones JE, Armando I, Jose PA. Role of renal DJ-1 in the pathogenesis of hypertension associated with increased reactive oxygen species production. *Hypertension*. 2012;59:446–452.
10. Cuevas S, Yang Y, Konkalmatt P, Asico LD, Feranil J, Jones J, Villar VA, Armando I, Jose PA. Role of nuclear factor erythroid 2-related factor 2 in the oxidative stress-dependent hypertension associated with the depletion of DJ-1. *Hypertension*. 2015;65:1251–1257.
11. Sreedhar A, Zhao Y. Uncoupling protein 2 and metabolic diseases. *Mitochondrion*. 2017;34:135–140.

12. Toral M, Romero M, Jimenez R, Robles-Vera I, Tamargo J, Martinez MC, Perez-Vizcaino F, Duarte J. Role of UCP2 in the protective effects of PPARbeta/delta activation on lipopolysaccharide-induced endothelial dysfunction. *Biochem Pharmacol*. 2016;110–111:25–36.

13. Diao JY, Wei J, Yan R, Lin L, Li H. Effect of uncoupling protein 2 on high-glucose induced mitochondrial damage and apoptosis of cardiomyocytes. *Zhonghua Yi Xue Za Zhi*. 2016;96:2493–2497.

14. Gero D, Szabo C. Glucocorticoids suppress mitochondrial oxidant production via upregulation of uncoupling protein 2 in hyperglycemic endothelial cells. *PLoS One*. 2016;11:e0154813.

15. Ji XB, Li XR, Hao D, Sun Q, Zhou Y, Wen P, Dai CS, Yang JW. Inhibition of uncoupling protein 2 attenuates cardiac hypertrophy induced by transverse aortic constriction in mice. *Cell Physiol Biochem*. 2015;36:1688–1698.

16. Patterson AD, Shah YM, Matsubara T, Krausz KW, Gonzalez FJ. Peroxisome proliferator-activated receptor alpha induction of uncoupling protein 2 protects against acetaminophen-induced liver toxicity. *Hepatology*. 2012;56:281–290.

17. Serviddio G, Bellanti F, Tamborra R, Rollo T, Capitanio N, Romano AD, Sastre J, Vendemiale G, Altomare E. Uncoupling protein-2 (UCP2) induces mitochondrial proton leak and increases susceptibility of non-alcoholic steatohepatitis (NASH) liver to ischaemia-reperfusion injury. *Gut*. 2008;57:957–965.

18. Wilcox CS. Effects of tempol and redox-cycling nitroxides in models of oxidative stress. *Pharmacol Ther*. 2010;126:119–145.

19. Yang Z, Asico LD, Yu P, Wang Z, Jones JE, Escano CS, Wang X, Quinn MT, Sibley DR, Romero GG, Felder RA, Jose PA. D5 dopamine receptor regulation of reactive oxygen species production, NADPH oxidase, and blood pressure. *Am J Physiol Regul Integr Comp Physiol*. 2006;290:R96–R104.

20. Ha SD, Ng D, Lamothe J, Valvano MA, Han J, Kim SO. Mitochondrial proteins Bnip3 and Bnip3L are involved in anthrax lethal toxin-induced macrophage cell death. *J Biol Chem*. 2007;282:26275–26283.

21. Mei Y, Zhang Y, Yamamoto K, Xie W, Mak TW, You H. FOXO3a-dependent regulation of Pink1 (Park6) mediates survival signaling in response to cytokine deprivation. *Proc Natl Acad Sci USA*. 2009;106:5153–5158.

22. Sweeney TE, Suliman HB, Hollingsworth JW, Piantadosi CA. Differential regulation of the PGC family of genes in a mouse model of *Staphylococcus aureus* sepsis. *PLoS One*. 2010;5:e11606.

23. Yano M, Yamamoto T, Nishimura N, Gotoh T, Watanabe K, Ikeda K, Garan Y, Taguchi R, Node K, Okazaki T, Oike Y. Increased oxidative stress impairs adipose tissue function in sphingomyelin synthase 1 null mice. *PLoS One*. 2013;8:e61380.

24. Ganapathy PS, Perry RL, Tawfik A, Smith RM, Perry E, Roon P, Bozard BR, Ha Y, Smith SB. Homocysteine-mediated modulation of mitochondrial dynamics in retinal ganglion cells. *Invest Ophthalmol Vis Sci*. 2011;52:5551–5558.

25. Li L, Pan R, Li R, Niemann B, Aurich AC, Chen Y, Rohrbach S. Mitochondrial biogenesis and peroxisome proliferator-activated receptor-gamma coactivator-1alpha (PGC-1alpha) deacetylation by physical activity: intact adipocytokine signaling is required. *Diabetes*. 2011;60:157–167.

26. Sale MM, Hsu FC, Palmer ND, Gordon CJ, Keene KL, Borgerink HM, Sharma AJ, Bergman RN, Taylor KD, Saad MF, Norris JM. The uncoupling protein 1 gene, UCP1, is expressed in mammalian islet cells and associated with acute insulin response to glucose in African American families from the IRAS Family Study. *BMC Endocr Disord*. 2007;7:1.

27. Young CN, Cao X, Guruju MR, Pierce JP, Morgan DA, Wang G, Iadecola C, Mark AL, Davisson RL. ER stress in the brain subfornical organ mediates angiotensin-dependent hypertension. *J Clin Invest*. 2012;122:3960–3964.

28. Lin W, Harding HP, Ron D, Popko B. Endoplasmic reticulum stress modulates the response of myelinating oligodendrocytes to the immune cytokine interferon-gamma. *J Cell Biol*. 2005;169:603–612.

29. Azfer A, Niu J, Rogers LM, Adamski FM, Kolattukudy PE. Activation of endoplasmic reticulum stress response during the development of ischemic heart disease. *Am J Physiol Heart Circ Physiol*. 2006;291:H1411–H1420.

30. Yang L, Sha H, Davisson RL, Qi L. Phenformin activates the unfolded protein response in an AMP-activated protein kinase (AMPK)-dependent manner. *J Biol Chem*. 2013;288:13631–13638.

31. Woo CW, Cui D, Arellano J, Dorweiler B, Harding H, Fitzgerald KA, Ron D, Tabas I. Adaptive suppression of the ATF4-CHOP branch of the unfolded protein response by toll-like receptor signalling. *Nat Cell Biol*. 2009;11:1473–1480.

32. Kirkman DL, Muth BJ, Ramick MG, Townsend RR, Edwards DG. The role of mitochondria derived reactive oxygen species in microvascular dysfunction in chronic kidney disease. *Am J Physiol Renal Physiol*. 2018;314:F423–F429.

33. Malhotra JD, Kaufman RJ. ER stress and its functional link to mitochondria: role in cell survival and death. *Cold Spring Harb Perspect Biol*. 2011;3:a004424.

34. van Vliet AR, Agostinis P. Mitochondria-Associated Membranes and ER Stress. *Curr Top Microbiol Immunol*. 2018;414:73–102.

35. Chiang CK, Hsu SP, Wu CT, Huang JW, Cheng HT, Chang YW, Hung KY, Wu KD, Liu SH. Endoplasmic reticulum stress implicated in the development of renal fibrosis. *Mol Med*. 2011;17:1295–1305.

36. Santos CX, Nabeebaccus AA, Shah AM, Camargo LL, Filho SV, Lopes LR. Endoplasmic reticulum stress and Nox-mediated reactive oxygen species signaling in the peripheral vasculature: potential role in hypertension. *Antioxid Redox Signal*. 2014;20:121–134.

37. Andres-Mateos E, Perier C, Zhang L, Blanchard-Fillion B, Greco TM, Thomas B, Ko HS, Sasaki M, Ischiropoulos H, Przedborski S, Dawson TM, Dawson VL. DJ-1 gene deletion reveals that DJ-1 is an atypical peroxiredoxin-like peroxidase. *Proc Natl Acad Sci USA*. 2007;104:14807–14812.

38. Radi R. Nitric oxide, oxidants, and protein tyrosine nitration. *Proc Natl Acad Sci USA*. 2004;101:4003–4008.

39. McCoy MK, Cookson MR. DJ-1 regulation of mitochondrial function and autophagy through oxidative stress. *Autophagy*. 2011;7:531–532.

40. Hao LY, Giasson BI, Bonini NM. DJ-1 is critical for mitochondrial function and rescues PINK1 loss of function. *Proc Natl Acad Sci USA*. 2010;107:9747–9752.

41. Lee H, Abe Y, Lee I, Shrivastav S, Crusan AP, Huttemann M, Hopfer U, Felder RA, Asico LD, Armando I, Jose PA, Kopp JB. Increased mitochondrial activity in renal proximal tubule cells from young spontaneously hypertensive rats. *Kidney Int*. 2014;85:561–569.

42. Hu F, Liu F. Mitochondrial stress: a bridge between mitochondrial dysfunction and metabolic diseases? *Cell Signal*. 2011;23:1528–1533.

43. Pellegrino MW, Nargund AM, Haynes CM. Signaling the mitochondrial unfolded protein response. *Biochim Biophys Acta*. 2013;1833:410–416.

44. Campos JC, Bozi LH, Bechara LR, Lima VM, Ferreira JC. Mitochondrial quality control in cardiac diseases. *Front Physiol*. 2016;7:479.

45. Rizzo M, Macario AJ, de Macario EC, Gouni-Berthold I, Berthold HK, Rini GB, Zummo G, Cappello F. Heat shock protein-60 and risk for cardiovascular disease. *Curr Pharm Des*. 2011;17:3662–3668.

46. Juwono J, Martinus RD. Does Hsp60 provide a link between mitochondrial stress and inflammation in diabetes mellitus? *J Diabetes Res*. 2016;2016:8017571.

47. Yuan J, Dunn P, Martinus RD. Detection of Hsp60 in saliva and serum from type 2 diabetic and non-diabetic control subjects. *Cell Stress Chaperones*. 2011;16:689–693.

48. Veereshwarayya V, Kumar P, Rosen KM, Mestril R, Querfurth HW. Differential effects of mitochondrial heat shock protein 60 and related molecular chaperones to prevent intracellular beta-amyloid-induced inhibition of complex IV and limit apoptosis. *J Biol Chem*. 2006;281:29468–29478.

49. Marino Gammazza A, Colangeli R, Orban G, Pierucci M, Di Gennaro G, Lo Bello M, D'Aniello A, Bucchieri F, Pomara C, Valentino M, Muscat R, Benigno A, Zummo G, de Macario EC, Cappello F, Di Giovanni G, Macario AJ. Hsp60 response in experimental and human temporal lobe epilepsy. *Sci Rep*. 2015;5:9434.

50. Jung T, Hohn A, Grune T. The proteasome and the degradation of oxidized proteins: Part II—protein oxidation and proteasomal degradation. *Redox Biol*. 2014;2:99–104.

51. Raynes R, Pomatto LC, Davies KJ. Degradation of oxidized proteins by the proteasome: distinguishing between the 20S, 26S, and immunoproteasome proteolytic pathways. *Mol Aspects Med*. 2016;50:41–55.

52. Hartl FU, Bracher A, Hayer-Hartl M. Molecular chaperones in protein folding and proteostasis. *Nature*. 2011;475:324–332.

53. Elwi AN, Lee B, Meijndert HC, Braun JE, Kim SW. Mitochondrial chaperone DnaJA3 induces Drp1-dependent mitochondrial fragmentation. *Int J Biochem Cell Biol*. 2012;44:1366–1376.

54. Lee B, Ahn Y, Kang SM, Park Y, Jeon YJ, Rho JM, Kim SW. Stoichiometric expression of mtHsp40 and mtHsp70 modulates mitochondrial morphology and cristae structure via Opa1L cleavage. *Mol Biol Cell*. 2015;26:2156–2167.

55. Youn CK, Kim J, Jo ER, Oh J, Do NY, Cho SI. Protective effect of tempol against cisplatin-induced ototoxicity. *Int J Mol Sci*. 2016;17:E1931.

56. Brand MD, Esteves TC. Physiological functions of the mitochondrial uncoupling proteins UCP2 and UCP3. *Cell Metab*. 2005;2:85–93.

57. Zhou Y, Cai T, Xu J, Jiang L, Wu J, Sun Q, Zen K, Yang J. UCP2 attenuates apoptosis of tubular epithelial cells in renal ischemia-reperfusion injury. *Am J Physiol Renal Physiol*. 2017;313:F926–F937.
58. Nedergaard J, Ricquier D, Kozak LP. Uncoupling proteins: current status and therapeutic prospects. *EMBO Rep*. 2005;6:917–921.
59. Zhang CY, Baffy G, Perret P, Krauss S, Peroni O, Grujic D, Hagen T, Vidal-Puig AJ, Boss O, Kim YB, Zheng XX, Wheeler MB, Shulman GI, Chan CB, Lowell BB. Uncoupling protein-2 negatively regulates insulin secretion and is a major link between obesity, beta cell dysfunction, and type 2 diabetes. *Cell*. 2001;105:745–755.
60. Toda C, Kim JD, Impellizzeri D, Cuzzocrea S, Liu ZW, Diano S. UCP2 regulates mitochondrial fission and ventromedial nucleus control of glucose responsiveness. *Cell*. 2016;164:872–883.
61. Echtay KS. Mitochondrial uncoupling proteins—what is their physiological role? *Free Radic Biol Med*. 2007;43:1351–1371.
62. de Bilbao F, Arsenijevic D, Vallet P, Hjelle OP, Ottersen OP, Bouras C, Raffin Y, Abou K, Langhans W, Collins S, Plamondon J, Alves-Guerra MC, Haguenauer A, Garcia I, Richard D, Ricquier D, Giannakopoulos P. Resistance to cerebral ischemic injury in UCP2 knockout mice: evidence for a role of UCP2 as a regulator of mitochondrial glutathione levels. *J Neurochem*. 2004;89:1283–1292.
63. Cannon B, Shabalina IG, Kramarova TV, Petrovic N, Nedergaard J. Uncoupling proteins: a role in protection against reactive oxygen species–or not? *Biochim Biophys Acta*. 2006;1757:449–458.
64. Mattiasson G, Shamloo M, Gido G, Mathi K, Tomasevic G, Yi S, Warden CH, Castilho RF, Melcher T, Gonzalez-Zulueta M, Nikolich K, Wieloch T. Uncoupling protein-2 prevents neuronal death and diminishes brain dysfunction after stroke and brain trauma. *Nat Med*. 2003;9:1062–1068.
65. Jiang L, Qiu W, Zhou Y, Wen P, Fang L, Cao H, Zen K, He W, Zhang C, Dai C, Yang J. A microRNA-30e/mitochondrial uncoupling protein 2 axis mediates TGF-beta1-induced tubular epithelial cell extracellular matrix production and kidney fibrosis. *Kidney Int*. 2013;84:285–296.
66. Echtay KS, Roussel D, St-Pierre J, Jekabsons MB, Cadenas S, Stuart JA, Harper JA, Roebuck SJ, Morrison A, Pickering S, Clapham JC, Brand MD. Superoxide activates mitochondrial uncoupling proteins. *Nature*. 2002; 415:96–99.
67. Turner JD, Gaspers LD, Wang G, Thomas AP. Uncoupling protein-2 modulates myocardial excitation-contraction coupling. *Circ Res*. 2010;106:730–738.
68. McCormack JG, Denton RM. Mitochondrial Ca^{2+} transport and the role of intramitochondrial Ca^{2+} in the regulation of energy metabolism. *Dev Neurosci*. 1993;15:165–173.
69. Motloch LJ, Larbig R, Gebing T, Reda S, Schwaiger A, Leitner J, Wolny M, Eckardt L, Hoppe UC. By regulating mitochondrial Ca^{2+}-uptake UCP2 modulates intracellular Ca^{2+}. *PLoS One*. 2016;11:e0148359.
70. Graier WF, Trenker M, Malli R. Mitochondrial Ca^{2+}, the secret behind the function of uncoupling proteins 2 and 3? *Cell Calcium*. 2008;44:36–50.
71. Himmel HM, Whorton AR, Strauss HC. Intracellular calcium, currents, and stimulus-response coupling in endothelial cells. *Hypertension*. 1993;21:112–127.
72. Dedkova EN, Ji X, Lipsius SL, Blatter LA. Mitochondrial calcium uptake stimulates nitric oxide production in mitochondria of bovine vascular endothelial cells. *Am J Physiol Cell Physiol*. 2004;286:C406–C415.